References

[1]Clark, B.L., "A Parametric Study of the Transient Ablation of Teflon," *Transations of the ASME, Ser. C: Journal of Heat Transfer,* Vol. 94, Nov. 1972, pp. 347-354.

[2]Vujanovic, B., "Application of Optimal Linearization Method to the Heat Transfer Problem," *International Journal of Heat and Mass Transfer,* Vol. 16, June 1973, pp. 1111-1117.

[3]Mastanaiah, K., "Approximate Solution of Transient Temperature Distribution in a Two-Layer Composite Slab," Internal Rept. SSTC/PSN:TP:1/72, April 1972, VSSC, Trivandrum, India.

[4]Jaakola, T.H. and Luus, R., "Optimization of Direct Search and Systematic Reduction of the size of Search Region," *AIChE Journal,* Vol. 19, July 1973, pp. 760-766.

Experimental Verification of Turbulent Skin Friction Reduction with Compliant Walls

Leonard M. Weinstein* and Michael C. Fischer†
NASA Langley Research Center, Hampton, Va.

and

Robert L. Ash‡
Old Dominion University, Norfolk, Va.

Nomenclature

a	= nondimensional amplitude parameter
C_f	= local skin friction coefficient
E	= Young's modulus
f_{vib}	= membrance fundamental vibration frequency
F_{peak}	= peak power frequency in turbulent spectra
L	= length
M_∞	= freestream Mach number
n	= power law exponent
P_t	= tunnel total pressure
q	= dynamic pressure
$\dot{q}$	= heating rate
R_x	= Reynolds number based on x
T_x	= membrance tension in x direction
T_z	= membrance tension in z direction
t	= material thickness
u	= velocity
w	= width
x	= distance in freestream flow direction from virtual origin
y	= distance perpendicular to model surface
z	= distance along model surface perpendicular to freestream flow direction
δ	= boundary-layer thickness
ρ	= density
τ	= shearing stress

Subscripts

rigid	= referred to rigid condition
ω	= referred to wall condition
∞	= referred to freestream condition

Superscripts

$-$	= time average value
$'$	= instantaneous value

Received December 11, 1974.

Index categories: Aircraft Structural Materials; Boundary Layers and Convective Heat Transfer—Turbulent; Subsonic and Transonic Flow.

*Aerospace Engineer, Applied Fluid Mechanics Section, High-Speed Aerodynamics Division.

†Special Assistant, Viscous Drag Reduction, Fluid Mechanics Branch, High-Speed Aerodynamics Division.

‡Associate Professor, School of Engineering.

BOUNDARY-LAYER skin friction drag on subsonic and supersonic aircraft accounts for approximately 50% and 40% respectively, of the total vehicle drag. Laminar (low skin friction) flow exists only near the leading-edge surfaces on typical transport aircraft, so that turbulent boundary-layer (high skin friction) flow is dominant on the vehicle. Since for subsonic jet transports, approximately half of the power required for cruise is necessary to overcome the skin friction drag, the potential savings in fuel, or gain in payload or range from even a moderate skin friction drag reduction, merits a re-evaluation of methods for reducing skin friction drag.

Kramer[1,2] is credited with the original idea of drag reduction by compliant surfaces, based on his observation of dolphins swimming in water. Kramer's experiments showed a drag reduction of approximately 50% for a towed compliant coated cylinder; however, these results are questionable.[3] A survey of both theoretical and experimental investigations of the compliant wall effect is given by Fischer and Ash.[3]

Total skin friction drag reductions of up to 50% have been reported by Blick and his co-workers[4] (see Ref. 3 for the numerous other investigations reported by Blick) in their studies of low-speed turbulent boundary-layer air flow over compliant surfaces. More recently, Mattout[5] conducted tests in water with passive and active (mechanically driven) compliant wall membrances and reported drag reductions of up to 20%. Tests recently completed by McAlister and Wynn[6] attempted to duplicate Blick's studies; however, they found no drag reduction.

Preliminary compliant wall test results obtained in the Low Turbulence Pressure Tunnel (LTPT) at Langley Research Center have shown promising results. Test conditions for this investigation covered a velocity range of 30-90 m/sec (P_t from 1.01×10^5-8.11×10^5 N×m^2) and Reynolds number range of 7.4×10^6-106×10^6 based on a calculated virtual origin 3.96 m ahead of the survey station. A rigid surface for reference comparison, as well as various compliant wall surfaces, 46.7 cm wide and 127 cm long, were flush mounted on the side wall of the tunnel. Hot wire mean velocity and Reynolds stress data were obtained at one survey station 12.7 cm upstream from the rear of each surface. Limitations in the survey mechanism travel prevented traversing to the boundary-layer edge, but boundary-layer thicknesses of 2.54-7.62 cm were deduced from velocity power law profile fits to the measured data.

All of the compliant surfaces tested except one consisted of 0.64 cm thick polyurethane foam with various surface coverings. Compliant surface skins consisted of 0.0025 cm thick mylar, stretched under tension and area (complete surface) bonded or longitudinally strip bounded with silicone rubber adhesive to the foam and in one case to the rigid surface. Other compliant surfaces consisted of smooth silicone rubber sheets area bonded to the foam. A tension of approximately 1.75 N/cm was applied to the mylar membrances prior to testing, but membrance "bowing" during testing due to a slight differential pressure probably increased the tension and produced visible air gaps in unbounded regions. Two 0.64 cm nominally thick foam substrates were used: 39 pores/cm (PPC) polyurethane foam and compressed 35 PPC polyurethane foam.

Mean velocity and fluctuating survey data were obtained with a single slanted hot wire, which was rotated to measure $\bar{u}'\bar{v}'$.[7] Since a single wire was used, matching two different wires was not required. The wire was inclined at approximately 45° with the plane of the wire aligned with the flow and perpendicular to the surface. The wire was used in two positions rotated 180° apart. Absolute measurements of Reynolds stress require angle-of-attack calibration of the probe. However, since these calibrations were not available, the present measurements were ratioed to values obtained on the reference (rigid) plate. The present relative Reynolds stress measurements are believed to be accurate within ± 5%.

The most effective compliant wall was the 0.0025 cm thick mylar membrance stretched under tension and area bonded to

the compressed foam substrate. Mean velocity profiles indicated up to a 20% reduction in boundary-layer thickness (and lower momentum thickness) for this compliant surface compared with the rigid surface. This reduction in boundary-layer thickness indicates a drag reduction has occurred. Complementing these mean profile results are the Reynolds stress measurements obtained in the boundary layer over the mylar/compressed foam surface which are shown in Fig. 1 for $u_\infty = 61$ m/sec and $R_x = 13.5 \times 10^6$. Shearing stresses for the rigid and compliant surface are presented, normalized by the rigid wall value determined by extrapolating the Reynolds stress measurements to the wall. A 16% reduction in wall shear is clearly evident for the mylar/compressor foam compliant surface, which was the most effective surface tested.

A summary of the Reynolds stress measurements obtained with all of the compliant surfaces tested, expressed as a wall shear normalized by the rigid value is presented in Fig. 2. On the average, the maximum drag reduction occurred at the intermediate velocity ($u_\infty = 61$ m/sec). Note that all of the compliant surfaces tested except one, the 0.081 cm silicone rubber bonded to 39 PPC foam, exhibited a skin friction reduction. This surface (0.081-cm silicone rubber on 39 PPC foam) was stiffer, less responsive to the touch, and tended to form low-frequency or standing waves. The surface response was therefore probably too slow for any "favorable" alteration of the turbulence structure. However, data from a recent study[8] indicate increased turbulent transport (higher $\dot{q}$/shear) when low-frequency disturbances are incident on a turbulent boundary layer, which may be similar in behavior to the 0.081 cm silicone rubber on 39 PPC foam.

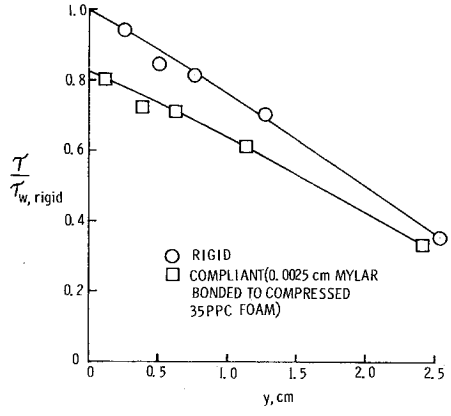

Fig. 1 Comparison of rigid and compliant surface shear stress determined from hot-wire Reynolds stress measurements; $u_\infty = 61$ m/sec, $R_x = 13.5 \times 10^6$.

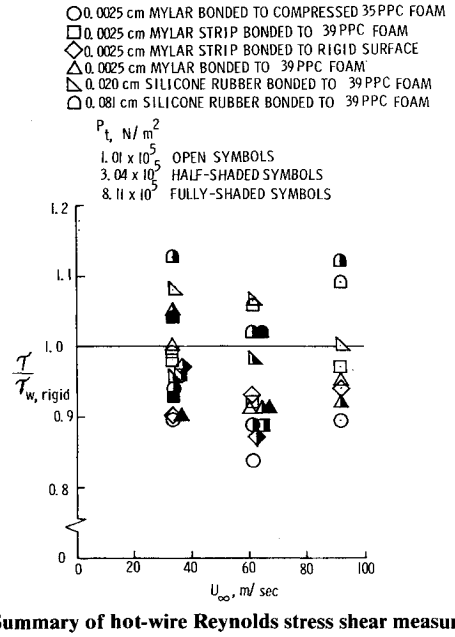

Fig. 2 Summary of hot-wire Reynolds stress shear measurements for all compliant surfaces examined.

In conjunction with Langley's program, a correlation developed by Ash[9] of existing membrance compliant wall data presented in Fig. 3 suggests that maximum skin friction reduction occurs when the fundamental membrance frequency, f_{vib}, is about half the power frequency in the boundary layer, f_{peak}, where, for a membrane[9]

$$f_{vib} = \left[\frac{T_y/w^2 + T_x/L^2}{\rho t} \right]^{1/2} \tag{1}$$

and from the energy spectrum for a typical turbulent flow

$$f_{peak} \simeq u_\infty / 2\pi\delta \tag{2}$$

The scatter of data in Fig. 3 indicate that even if the frequency is in the correct band, the vibration amplitude can produce either a roughness dominated drag-increasing effect if it is too large or no effect if it is too small.

For the present mylar/compressed 35 PPC foam and mylar/39 PPC foam compliant suurfaces, a vibration frequency was estimated by assuming the bonded membrance surface did not alter the frequency response of the elastic slab, in which case the first mode plane response frequency of the slab substrate was

$$f_{vib} = (1/4)\ (E/\rho)^{1/2} \tag{3}$$

It is recognized that this assumption for compliant slab vibration frequency is simplified, but because of the thinness of the membrane, Eq. (3) should give reasonable values.

Using Eqs. (2) and (3), mylar/foam frequency data for the present study were calculated and are presented in Fig. 3. Based on the assumed frequency analysis, it appears that the vibration frequencies were too high by factors of about 1.5-20 (see Fig. 3). To provide a means for assessing relative surface displacements, an amplitude parameter was deduced from the material and flow properties as

$$a \simeq qt/\delta E \tag{4}$$

Data for the present study with amplitude parameters a of the same magnitude are connected by lines (see Fig. 3) and suggest that in these cases the amplitude may have been of the correct order, even though the frequency was apparently too high for optimum drag reduction.

In conclusion, the preliminary results presented herein are promising, particularly since "unoptimized" surfaces were utilized in this initial investigation. Comprehensive tests with

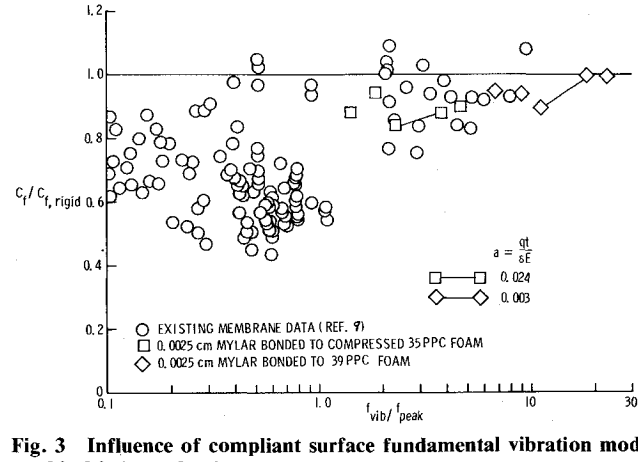

Fig. 3 Influence of compliant surface fundamental vibration mode on skin friction reduction.

the mylar/foam surface are planned to obtain detailed hot-wire, pitot, and surface displacement measurements at numerous survey stations along the compliant wall. Other promising surfaces will also be examined experimentally as an integral part of a continuing theoretical, experimental, and materials program to understand the drag reducing mechanism and to analyze the frequency, amplitude, and vibrational behavior of low-modulus materials. The ultimate goal is to develop practical and durable compliant surfaces optimized for maximum drag reduction, with applications to the fuselage of the next generation of subsonic/supersonic transports and possible application as a retrofit to existing transports. It should be noted that the present data are the first compliant wall test results at dynamic pressure corresponding to flight conditions of subsonic transport aircraft.

References

[1] Kramer, M. O., "Boundary Layer Stabilization by Distributed Damping," *Journal of the American Society of Naval Engineers*, Vol. 72, Feb. 1960, pp. 25-30.

[2] Kramer, M. O., "Dolphins' Secret," *Journal of the American Society of Naval Engineers*, Vol. 73, Feb. 1961, pp. 103-107.

[3] Fischer, M. C. and Ash, R. L., "A General Review of Concepts for Reducing Skin Friction, Including Recommendations for Future Studies," TM X-2894, March 1974, NASA.

[4] Blick, E. F., Walters, R. R., Smith, R., and Chu, H., "Compliant Coating Skin Friction Experiments," AIAA Paper 69-165, New York, N.Y., 1969.

[5] Mattout, R., "Reduction de trainee par parois souples" (Reduction of Drag by Flexible Walls), Bulletin No. 72, 1972, Association Technique Maritime et Aeronautique, pp. 207-227.

[6] McAlister, K. W. and Wynn, T. M., "Experimental Evaluation of Compliant Surfaces at Low Speeds," TM X-3119, Oct. 1974, NASA.

[7] Fujita, H. and Kovasznay, L. S., "Measurement of Reynolds Stress by a Single Rotated Hot-Wire Anemometer," *The Review of Scientific Instruments*, Vol. 39, Sept. 1968, pp. 1351-1355.

[8] Gougat, P., "External Sound Field Effect on a Turbulent Layer," TTF-15,852, July 1974, NASA.

[9] Ash, R. L., "On the Theory of Compliant Wall Drag Reduction in Turbulent Boundary Layers," CR 2387, April 1974, NASA.

Supersonic Flutter of Parallel Flat Plates Connected by an Elastic Medium

D. J. Johns*

University of Technology, Loughborough, U.K.

Introduction

THE configuration to be analyzed is shown in Fig. 1 and consists of an upper isotropic plate over which there is a supersonic air flow, separated by a linear elastic medium from a lower isotropic plate which may have different material properties and in-plane loadings from the upper plate. All plate edges are assumed to be simply-supported.

The flutter behavior of this configuration was investigated in Ref. 1 using a "static" supersonic strip theory in a two-mode Galerkin approach and sufficient graphical results were presented to indicate that the elastic connecting medium could have significant effects which depended also on the values of the in-plane loads.

The purpose of this Note is to present analyses based on a similar approach, and also on the use of a finite difference procedure, but using linear piston theory, and from which the influences of the various parameters can more readily be identified. Comparisons are made with the results of Ref. 1 and, for the case of the lower plate rigid, with Ref. 2.

Received December 16, 1974.

Index category: Aeroelasticity and Hydroelasticity.

*Professor and Head of Department of Transport Technology. Associate Fellow AIAA.

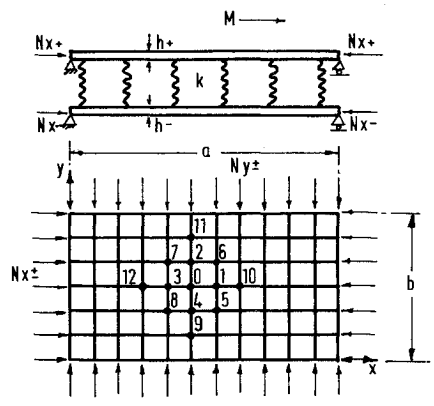

Fig. 1 Configuration and coordinate system showing finite difference mesh.

Governing Equations

The governing differential equations and boundary conditions are[1]

$$D_+\nabla^4 w_+ + N_{x+}\cdot(\partial^2 w_+/\partial x^2) + N_{y+}\cdot(\partial^2 w_+/\partial y^2) + \delta_+ h_+(\partial^2 w_+/\partial t^2) + k(w_+ - w_-) = L_{(w_+)} \quad (1)$$

$$D_-\nabla^4 w_- + N_{x-}(\partial^2 w_-/\partial x^2) + N_{y-}(\partial^2 w_-/\partial y^2) + \delta_- h_-(\partial^2 w_-/\partial t^2) + k(w_- - w_+) = 0 \quad (2)$$

$$w\pm(x,o,t) = w\pm(x,b,t) = w\pm(o,y,t) = w\pm(a,y,t) = 0$$

$$(\partial^2 w\pm/\partial y^2)(x,o,t) = (\partial^2 w\pm/\partial y^2)(x,b,t) = (\partial^2 w\pm/\partial x^2)(o,y,t) = (\partial^2 w\pm/\partial x^2)(a,y,t) = 0 \quad (3)$$

The subscripts $\pm$ refer to upper and lower plate, respectively, and all other notation is standard and as in Ref. 1.

In Eq. (1) the lateral aerodynamic pressure L is represented by the following simple expression from linear piston theory

$$L = -[P_1\dot{w}_+ + (P_2/a)w'_+] \quad (4)$$

where the prime and dot denotes a differentiation with respect to (x/a) and time (t), respectively. Clearly $P_1 = 0$ when aerodynamic damping is neglected.

Structural damping has not been considered in general. However hysteretic damping in the connecting medium can be represented by $k_g = k(1+ig)$.

Galerkin Procedure

If assumed functions $X\pm$ and $Y\pm$ are substituted into Eqs. (1) and (2), then these equations are not, in general, satisfied identically, and the Galerkin method may be invoked. It can easily be shown that for simply supported edges and the assumption of trigonometric functions, the chordwise modes (in x) and the spanwise modes (in y) must be similar for the upper and lower plates for a coupled plate solution to be possible.

Based on the two modes

$$w\pm = C_{mn\pm}\sin\left(\frac{m\pi x}{a}\right)\sin\left(\frac{n\pi y}{b}\right) + C_{rn\pm}\sin\left(\frac{r\pi x}{a}\right)\sin\left(\frac{n\pi y}{b}\right) \quad (5)$$